

Evaluation of a Predictive Constitutive Model for Sands

José E. Andrade, A.M.ASCE¹; and Kirk C. Ellison, S.M.ASCE²

Abstract: In this technical note, an evaluation of the robustness and predictive ability of a constitutive model for sands is performed. The model is shown to capture the main features of sand behavior under both drained and undrained monotonic loadings for a wide range of relative densities and stress paths. The main contribution of this technical note is to evaluate a robust, yet simple, constitutive framework based on a solid theoretical basis that fulfils the most fundamental requirement of any useful constitutive law: accurate predictions.

DOI: 10.1061/(ASCE)1090-0241(2008)134:12(1825)

CE Database subject headings: Sand; Constitutive models; Loads; Predictions; Soil properties; Parameters.

Introduction

In this technical note, a simplified version of the model developed by Borja and Andrade (2006) and Andrade and Borja (2006) is evaluated. The constitutive model is an offspring of the rigid-plastic model proposed by Jefferies (1993) with several improvements, including crucial features such as: a hyperelastic region, bulk and shear moduli dependent on the effective pressure, dependence of plastic flow on all three stress invariants, nonassociativity, and large deformations capabilities. The model has been successfully implemented into a general purpose finite element code and has been coupled with fluid flow to perform simulations of fully saturated sands under plane strain compression (Andrade and Borja 2007). The behavior of loose sands under undrained conditions and the occurrence of liquefaction instabilities have been explored in detail in Andrade (2008). The ability of the model to predict the onset of liquefaction or phase transformation has also been established.

For the calibrations and predictions presented herein, the model has been simplified to an associative formulation to reduce the number of constitutive parameters that must “fit” to the data. In summary, the simplified version of the model adheres to thermodynamical laws [e.g., the dissipation inequality, see Borja and Andrade (2006) for more details] and requires a total of nine material parameters listed in Table 1. Out of these parameters, those pertaining to elasticity and critical state soil mechanics (CSSM) are standard and their evaluation is relatively straightforward if adequate experimental data are available. Further, the preconsolidation pressure can be obtained from the overconsolidation ratio (OCR) and the ellipticity is related to the friction angle. The curvature of the yield surface N and the hardening modulus h are perhaps the least physical of the parameters

and require direct calibration. However, in the subsequent sections we will show that calibration may be performed using a few force–displacement curves and then the same material parameters can be used to predict the material behavior.

Calibration and Predictions

The ability of the constitutive model to capture sand behavior will be demonstrated herein through the emulation of experimental data for three types of sand under a variety of monotonic loading conditions. The predictive ability of the model will also be exhibited for two of these data sets by using the calibrated parameters to predict soil behavior for additional loading conditions.

Calibration and Predictions for Brasted Sand (Cornforth 1964)

The Brasted sand data set consists of a total of four tests on loose ($e_0 \approx 0.75$) and dense ($e_0 \approx 0.57$) specimens, each under both triaxial compression (CTC) and plane strain compression loading. For the loose specimens, the coefficient of lateral earth pressure after consolidation is $K_0 = 0.45$, the mean normal effective stress after consolidation is $p_0 = 390$ kPa, the initial preconsolidation pressure is $p_c = 715$ kPa and the hardening parameter $h = 70$. For the dense specimens, $K_0 = 0.38$, $p_0 = 425$ kPa, $p_c = 1150$ kPa, and $h = 120$. These paired data sets isolate the effect of the stress path for a given soil density, as well as the effect of density for a given loading condition. The parameters were calibrated under triaxial compression and then applied to make genuine predictions of the sand behavior under plane strain compression.

The parameters M and μ_0 were determined from the residual and elastic portions of the data plots, respectively. The remaining parameters, including the critical state parameters, were calibrated to fit the data. As the stress path for triaxial compression meets the yield surface at a compression corner in the deviatoric plane, any value for the parameter ρ would have yielded the same model response. The writers chose to select a value of 0.78 for ρ because this value closely approximates the Mohr–Coulomb yield surface, which has previously been validated through many phenomenological studies (Lade and Duncan 1975; Matsuoka and Nakai 1982). Besides the initial void ratio e_0 specified by Cornforth (1964), only the parameters, p_c and h , were allowed to vary be-

¹Professor, Dept. of Civil and Environmental Engineering, Northwestern Univ., Evanston, IL 60208-3109 (corresponding author). E-mail: j-andrade@northwestern.edu

²Graduate Student, Dept. of Civil and Environmental Engineering, Northwestern Univ., Evanston, IL 60208-3109.

Note. Discussion open until May 1, 2009. Separate discussions must be submitted for individual papers. The manuscript for this technical note was submitted for review and possible publication on August 31, 2007; approved on April 4, 2008. This technical note is part of the *Journal of Geotechnical and Geoenvironmental Engineering*, Vol. 134, No. 12, December 1, 2008. ©ASCE, ISSN 1090-0241/2008/12-1825–1828/\$25.00.

Table 1. Summary of Material Parameters for Constitutive Model

Symbol	Parameter	Theory
μ_0	Shear modulus	Elasticity
κ	Gradient of swelling	CSSM
v_{c0}	Reverence specific volume	CSSM
λ	Compression gradient	CSSM
M	CSL slope on meridian plane	CSSM
N	Curvature of yield surface	Plasticity
ρ	Ellipticity	Plasticity
p_c	Preconsolidation pressure	Plasticity
h	Hardening constant	Plasticity

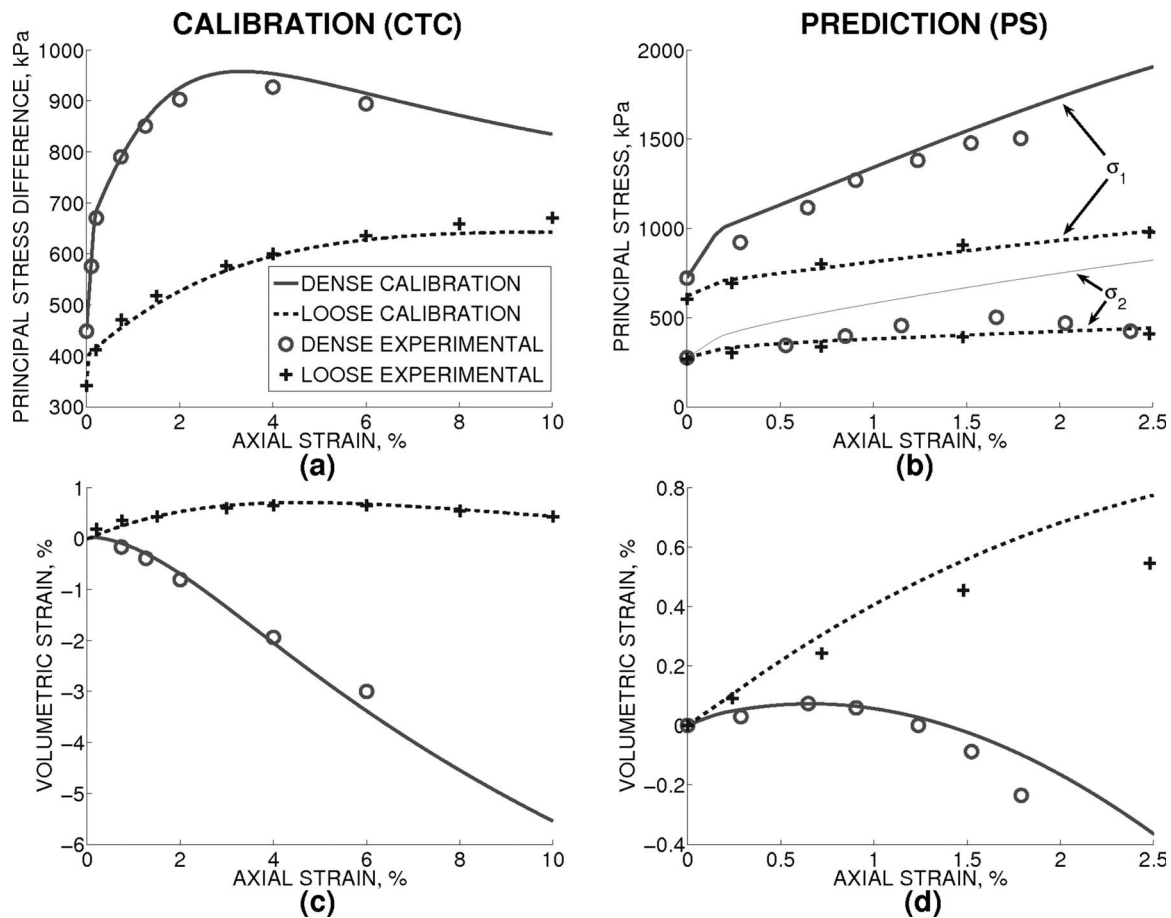
Table 2. Summary of Elastic and Plastic Parameters for Brasted, Monterey No. 0, and Hostun Sand Specimens

	Monterey sand	Brasted sand	Hostun sand
μ_0 (kPa)	40,000	45,000	40,000
κ	0.0010	0.0015	0.0020
v_{c0}	1.8250	1.8911	1.8920
λ	0.013	0.020	0.020
M	1.30	1.27	1.00
N	0.50	0.40	0.10
ρ	0.78	0.78	0.78

tween the loose and dense specimens during calibration of the model under triaxial compression. The final parameter selections are summarized in Table 2.

The model calibration in triaxial compression and the model predictions in plane strain are shown side-by-side in Fig. 1. Figs. 1(a and c) show that the model was able to capture the triaxial compression behavior quite well for both the loose and dense specimens. The plane strain predictions in Figs. 1(b and d) also show reasonably close agreement with the experimental data to an axial strain of approximately 2%. Discrepancies between the plane strain data and the model predictions include slight overpredictions of compressive volumetric strain in Fig. 1(d) and overprediction of the intermediate principal stress for the dense sand specimen in Fig. 1(b).

It is important to note that the postpeak behavior for dense sand specimens are not purely constitutive and will depend on the boundary conditions when implemented in a finite element framework due to the phenomenon of shear banding. Although this observation applies to any loading condition, shear bands occur more easily under plane strain conditions. The purely constitutive relation implies that the principal stresses will continue to increase with axial strain during plane strain compression long after a shear band is likely to have formed in the corresponding laboratory simulation; however, the formation of a shear band in finite element simulations allows for more realistic peak and postpeak responses (Andrade et al. 2008; Andrade and Borja 2006). As this

**Fig. 1.** (a) and (c) drained triaxial compression calibrations; and (b) and (d) drained plane strain compression predictions versus experimental data for loose and dense Brasted sand specimens

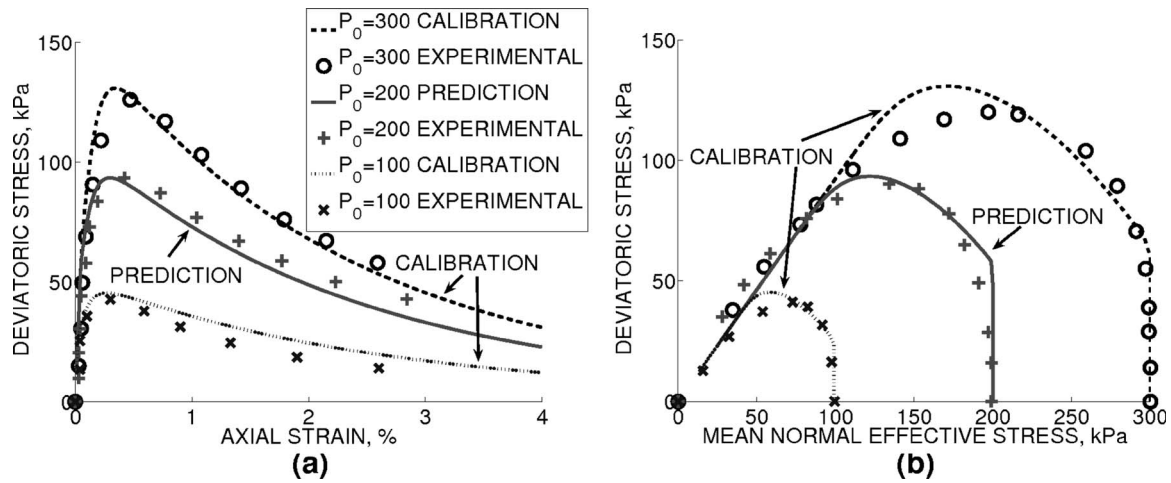


Fig. 2. Model calibration and prediction of static liquefaction versus experimental data for undrained triaxial compression testing of very loose Hostun Sand

technical note seeks only to evaluate the constitutive model, the comparison of plane strain predictions with laboratory data are cut off at an axial strain of 2.5%.

Calibration Prediction for Hostun Sand (Doanh et al. 1997)

This data set is composed of three undrained triaxial compression tests on very loose Hostun Sand. All three tests were isotropically consolidated to a void ratio of 1.0 before shearing. The preconsolidation pressure for each test was determined based on an overconsolidation ratio, $OCR=1.25$, and the hardening parameter was calibrated to $h=100$. Thus, the only condition that changes between the tests is the initial mean normal stress p_0 after consolidation. The model was calibrated to fit experimental data when $p_0=99$ and 300 kPa, and then the calibrated parameters were used to predict behavior for the $p_0=200$ kPa experiment. Only one test would have been necessary to calibrate the model if the critical state parameters were already known. However, in the experience of the writers, a variety of close fits can be obtained for a single test by trade-offs between the yield surface parameters, ρ and N , and the critical state parameters, v_{c0} , λ , and κ . Therefore, it is recommended that the calibration be performed for at least two tests if the true critical state parameters are unavailable.

With the Hostun Sand data set, the model attempts to capture a nonlinear stress path in addition to the corresponding stress-strain relations. Fig. 2 shows close agreement between the experimental data, model calibrations, and model prediction. Thus, the ability of the model to emulate and predict sand behavior is demonstrated again. One notable discrepancy between the model predictions and the experimental data is that the stress reversal points obtained from the model in Fig. 2(b) all occur at lower values of mean normal effective stress, p , than were observed in the experiments. In addition, the values of p predicted by the model are constant in the elastic region and, therefore, overstated near the beginning of the simulations.

Although the model's ability to predict static liquefaction has been demonstrated in Fig. 2, Andrade (2008) demonstrates that the model is also able to capture phase transformation during undrained loading, whereby a specimen momentarily appears to be approaching a peak deviatoric stress, but ultimately avoids

liquefying. The interested reader is directed to Andrade (private communication, 2007) for a discussion of the model's ability to describe this phenomenon.

True Triaxial Calibration for Monterey No. 0 Sand (Lade and Kim 1988)

Although many constitutive models are able to capture soil behavior for a given loading condition, fewer models succeed in replicating experimental data from a variety of stress paths. Therefore, the robustness of this model was verified using true triaxial data for Monterey No. 0 Sand (Lade and Kim 1988). The samples were compacted to a relative density of approximately 98% ($e_0 \approx 0.55$), isotropically consolidated to 60 kPa and then sheared along a variety of linear stress paths. The preconsolidation pressure was set to $p_c=200$ kPa and the hardening parameter was set to $h=500$. As the consolidation histories were identical for each test, this data set highlights the effect of the loading conditions on the soil response. The stress path for each test is described by a B value, where

$$B = \frac{\sigma_2 - \sigma_3}{\sigma_1 - \sigma_3} \quad (1)$$

The minor stress, σ_3 , was held constant for each test; therefore, $B=0.0$ represents CTC and $B=1.0$ represents triaxial extension.

As the initial conditions prior to shearing were identical for each test, the model parameters were likewise identical for each computation. The critical state parameters, λ , κ , and v_{c0} , deviate only slightly from published values (Collins et al. 1992). The initial void ratio, e_0 , and the critical state stress ratio, M , were also selected based on published values of minimum void ratio e_{\min} , maximum void ratio e_{\max} , and the critical state friction angle ϕ_{cs} (Collins et al. 1992). The initial shear modulus μ_0 , was calculated directly from the available data. The preconsolidation pressure p_c , the plastic modulus h , and the yield surface parameters, N and ρ , were all selected to fit the data. The model parameters for this data set are summarized in Table 2.

Fig. 3 shows close agreement between the calibrated model predictions and the experimental data. Although the principal stress difference for $B=0$ is underpredicted in Fig. 3(a), and the

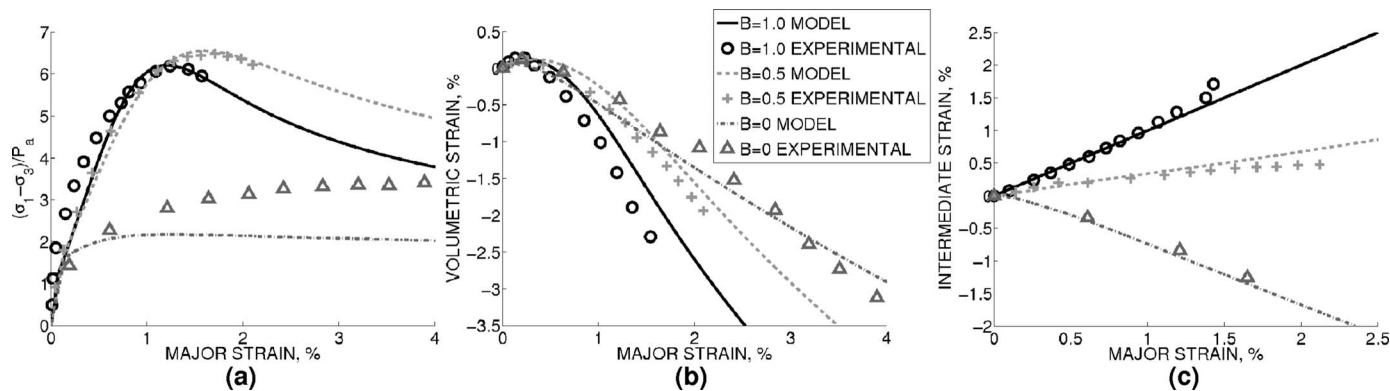


Fig. 3. Experimental data and model calibrations for drained true triaxial testing of dense Monterey No. 0 Sand

volumetric strain is slightly underpredicted for $B=0.5$ and 1.0 in Fig. 3(b), the model does a decent job of capturing the sand behavior overall. Further, the model does an exceptional job of capturing the relations between the principal strains in Fig. 3(c).

Conclusions

A simple, robust, and predictive constitutive model for sands has been evaluated that adheres to thermodynamical laws and solid mechanical theories, simultaneously being amenable to numerical implementation. The robustness of the model was demonstrated by replicating three data sets that utilized experimental results to calibrate the model parameters. These data sets represented a wide variety of stress paths under drained and undrained monotonic loading conditions. The true power of the model, however, has been demonstrated by accurate predictions for two data sets. Since the experimental results were not considered when making the predictions, they can tacitly be interpreted as though the predictions were made prior to the actual event. The model's ability to not only capture sand behavior, but also to predict it, shows promise for its effective use in more intricate, larger-scale finite element analyses.

Acknowledgments

This work is partially supported by NSF Grant No. CMMI-0726908 to Northwestern University and is gratefully acknowledged. Also, the second writer would like to acknowledge the partial support of his MS studies at Northwestern via a Walter P. Murphy Graduate Fellowship.

References

- Andrade, J. E. (2008). "A predictive framework for liquefaction instability." *Geotechnique*, in press.
- Andrade, J. E., Baker, J. W., and Ellison, K. C. (2008). "Random porosity fields and their influence on the stability of granular media." *Int. J. Numer. Analyt. Meth. Geomech.*, 32, 1147–1172.
- Andrade, J. E., and Borja, R. I. (2006). "Capturing strain localization in dense sands with random density." *Int. J. Numer. Methods Eng.*, 67, 1531–1564.
- Andrade, J. E., and Borja, R. I. (2007). "Modeling deformation banding in dense and loose fluid-saturated sands." *Finite Elem. Anal. Design*, 43, 361–383.
- Borja, R. I., and Andrade, J. E. (2006). "Critical state plasticity. Part VI: Meso-scale finite element simulation of strain localization in discrete granular materials." *Comput. Methods Appl. Mech. Eng.*, 195, 5115–5140.
- Collins, I. F., Pender, M. J., and Wang, Y. (1992). "Cavity expansion in sands under drained loading conditions." *Int. J. Numer. Analyt. Meth. Geomech.*, 16, 3–23.
- Cornforth, D. H. (1964). "Some experiments on the influence of strain conditions on the strength of sand." *Geotechnique*, 14, 143–167.
- Doanh, T., Ibrahim, E., and Matiotti, R. (1997). "Undrained instability of very loose hostun sand in triaxial compression and extension. Part I: Experimental observations." *Mech. Cohesive-Frict. Mater.*, 2, 47–70.
- Jefferies, M. G. (1993). "Nor-sand: A simple critical state model for sand." *Geotechnique*, 43, 91–103.
- Lade, P. V., and Duncan, J. M. (1975). "Elastoplastic stress-strain theory for cohesionless soil." *J. Geotech. Engrg. Div.*, 101, 1037–1053.
- Lade, P. V., and Kim, M. K. (1988). "Single hardening constitutive model for frictional materials II. Yield criterion and plastic work contours." *Comput. Geotech.*, 6, 13–29.
- Matsuoka, H., and Nakai, T. (1982). "A new failure criterion for soils in three-dimensional stresses." *Conf. on Deformation and Failure of Granular Materials*, International Union of Theoretical and Applied Mechanics (IUTAM), 253–263.